A 2D MODEL OF ULTRASONIC TESTING FOR CRACKS NEAR A NONPLANAR SURFACE

Jonathan Westlund and Anders Boström

Department of Applied Mechanics, Chalmers University of Technology,
SE-412 96 Göteborg, Sweden

ABSTRACT. 2D P-SV elastic wave scattering by a crack near a non-planar surface is investigated. The wave scattering problem is solved in the frequency domain using a combination of the boundary element method (BEM) for the back surface displacement and a Fourier series expansion of the crack opening displacement (COD). The model accounts for the action of the transmitting and receiving ultrasonic contact probes, and the time traces are obtained by applying an inverse temporal Fourier transform.

Keywords: Ultrasonics, Modeling, Crack, BIE, BEM.
PACS: 43.20.Gp, 43.20.Rz, 43.35.Zc.

INTRODUCTION

The propagation of elastic waves and scattering by defects have important applications in non-destructive testing (NDT) and evaluation (NDE), for instance in the nuclear power and aero-space industries. The most important and critical defect is a crack and a lot of work has been done on the scattering by cracks. However, not so much effort has been put into the modeling of the whole NDT situation, including also models of ultrasonic probes in transmission and reception. The purpose of the present work is to model the whole NDT situation in the cases when a crack in a thick-walled component is located close to a non-planar back surface, i.e. the surface opposite to the scanning surface. This is a situation that occurs in applications such as the testing of thick-walled pipes with a diameter change or a connection, in the nuclear power industry. The combination of a crack and a non-planar back surface complicates the ultrasonic testing because the signal from the crack may be masked by the signal from the non-planar surface. The 2D in-plane case is considered in this paper and this is an extension of the earlier work by Westlund [1], where the corresponding antiplane case is studied. The employed solution method is based on a reformulation of the wave scattering problem as a combination of a displacement boundary integral equation (BIE) for the back surface displacement and a hypersingular traction BIE for the crack opening displacement. This gives a very effective treatment of the crack while allowing a general geometry of the back surface, and since the method is essentially exact the model provides accurate results for both high and low frequencies.

CP1211, *Review of Quantitative Nondestructive Evaluation Vol.29,*
edited by D. O. Thompson and D. E. Chimenti

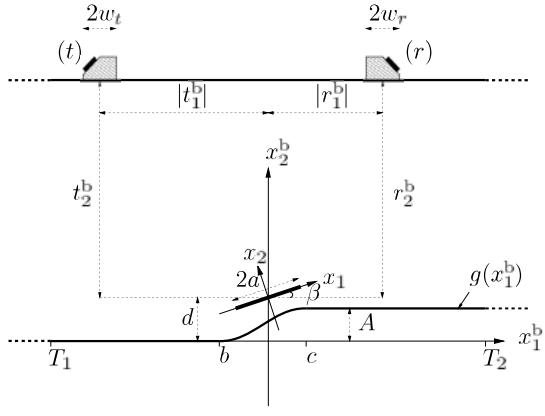

FIGURE 1. The geometry with an interior crack in a component with a non-planar back surface.

PROBLEM FORMULATION

Consider a 2D scattering geometry as depicted in Fig. 1, where an interior strip-like crack of width $2a$ is located in a thick-walled component with a non-planar back surface. In the exterior of the crack the component is isotropic and homogeneous with Lamé constants λ and μ and density ρ. The inclination of the crack with respect to the horizontal is given by the angle β.

Figure 1 also introduces two coordinate systems: the crack coordinate system (x_1, x_2) and the back surface coordinate system $(x_1^{\mathrm{b}}, x_2^{\mathrm{b}})$. The superscript 'b' on quantities indicate that they are represented in the back surface coordinate system. The standard transformation rules for the transformation between the two coordinate systems apply.

On the scanning surface of the component two ultrasonic contact probes are located: a transmitting ultrasonic probe (t) and a receiving ultrasonic probe (r). The half-widths of the probes are denoted w_t and w_r, respectively, and the positions of the probes in relation to the crack center are given by $(t_1^{\mathrm{b}}, t_2^{\mathrm{b}})$ and $(r_1^{\mathrm{b}}, r_2^{\mathrm{b}})$ in the coordinate system of the back surface. As a special case one probe can act as both transmitter and receiver in a pulse-echo testing situation.

The multiple scattering between the crack and the back surface is accounted for in the model, so the distance between them may be arbitrary as long as the crack is interior and not surface-breaking. However, the distance between the scanning surface of the component and the crack and back surface is assumed to be large enough (i.e. at least a couple of wavelengths) so that multiple scattering between these surfaces can be neglected.

To enable the subsequent boundary element discretization of the back surface, it is truncated at the left and right truncation limits T_1 and T_2. The actual shape of the non-planar back surface $g(x_1^{\mathrm{b}})$ may be quite arbitrary as long as it has no cusps, as scattering by such cusps is not accounted for. The back surface is assumed to be planar to the left of b and to the right of c, and A is the vertical distance between the lower and upper parts of the back surface.

In 2D elastodynamics the wave motion decouples into two types: in-plane P and SV waves and antiplane SH waves. In this paper the coupled P-SV wave scattering problem is treated. Time-harmonic conditions are considered, and the time-factor $\mathrm{e}^{-\mathrm{i}\omega t}$ is suppressed

throughout (where ω is the angular frequency and t the time). Under these conditions, the equations of motion are:

$$k_p^{-2}\nabla(\nabla\cdot\boldsymbol{u}) - k_s^{-2}\nabla\times(\nabla\times\boldsymbol{u}) + \boldsymbol{u} = \mathbf{0}, \tag{1}$$

where $k_p = \omega/c_p$ is the pressure wave number, $c_p = \sqrt{(\lambda+2\mu)/\rho}$ the pressure wave speed, $k_s = \omega/c_s$ the shear wave number and $c_s = \sqrt{\mu/\rho}$ the shear wave speed.

The crack is open and thus traction-free, and the back surface is also free of tractions. In addition, the scanning surface of the component is free of tractions except for the action of the ultrasonic probes which is discussed in a separate section. Letting C_{BS} denote the back surface, $\mathbf{e}_2$ the unit normal vector in the 2-direction of the coordinate system of the crack and $\mathbf{n}$ the downward unit normal vector on C_{BS}, the boundary conditions on the crack and back surface are thus:

$$\begin{cases} \lim\limits_{x_2\to 0^+}\boldsymbol{\sigma}(\boldsymbol{x})\cdot\mathbf{e}_2 = \lim\limits_{x_2\to 0^-}\boldsymbol{\sigma}(\boldsymbol{x})\cdot\mathbf{e}_2 = \mathbf{0}, & |x_1| < a \\ \boldsymbol{\sigma}(\boldsymbol{x})\cdot\mathbf{n} = \mathbf{0}, & (x_1,x_2)\in C_{BS}. \end{cases} \tag{2}$$

It should be noted that since $\boldsymbol{u}$ is discontinuous across the crack the boundary condition on the crack must be taken as a limit as the point approaches the crack, from either side.

THE INTEGRAL EQUATIONS

The solution method employed in this paper reformulates the wave scattering problem as two coupled boundary integral equations, which are subsequently solved simultaneously. The reformulation is based on the use of the outward propagating Green's displacement tensor for the infinite plane, denoted $\boldsymbol{U}^k(\boldsymbol{x},\boldsymbol{y};\omega)$ with corresponding Green's stress tensor $\boldsymbol{\Sigma}^k(\boldsymbol{x},\boldsymbol{y};\omega) = \boldsymbol{\mathcal{C}} : \nabla\boldsymbol{U}^k(\boldsymbol{x},\boldsymbol{y};\omega)$, where $\boldsymbol{\mathcal{C}}$ is the elastic stiffness tensor. Here and throughout, the ∇-operator always acts on the $\boldsymbol{x}$-coordinates unless otherwise specified. The Green's tensor, also called the Helmholtz fundamental solution in plane strain, is the outward propagating solution to the equation of motion (1) with a Dirac delta source term in the $\mathbf{e}_k$-direction of the coordinate system of the crack on the right-hand side. This Green's tensor can be given both in closed form in terms of Hankel functions [2] and on Fourier integral representation form by using Fourier integral representations of Hankel functions.

The regularization of the back surface integral equation makes use of the static Green's displacement tensor for the infinite plane, denoted $\boldsymbol{U}^k(\boldsymbol{x},\boldsymbol{y})$ with corresponding static Green's stress tensor $\boldsymbol{\Sigma}^k(\boldsymbol{x},\boldsymbol{y}) = \boldsymbol{\mathcal{C}} : \nabla\boldsymbol{U}^k(\boldsymbol{x},\boldsymbol{y})$. The static Green's tensor, also called the Kelvin fundamental solution in plane strain, is given explicitly by e.g. Bonnet [2].

The integral equation for the back surface is derived using the 2D divergence theorem, and is regularized by subtracting and adding back appropriate terms. The derivation and regularization are similar to the antiplane case [1], so the details are not given here. The result is the following integral equation for the back surface:

$$\begin{aligned} &-\int_{C_{BS}} u_i(\boldsymbol{x})\left[\Sigma_{ij}^k(\boldsymbol{x},\boldsymbol{y};\omega) - \Sigma_{ij}^k(\boldsymbol{x},\boldsymbol{y})\right]\mathrm{n}_j(\boldsymbol{x})\,\mathrm{d}s_x \\ &-\int_{C_{BS}} \left[u_i(\boldsymbol{x}) - u_i(\boldsymbol{y})\right]\Sigma_{ij}^k(\boldsymbol{x},\boldsymbol{y})\mathrm{n}_j(\boldsymbol{x})\,\mathrm{d}s_x - \frac{1}{2}u_k(\boldsymbol{y}) \\ &+\int_{-a}^{a}\Delta u_i(x_1)\Sigma_{i2}^k(x_1,0,\boldsymbol{y};\omega)\,\mathrm{d}x_1 + u_k^{\mathrm{in}}(\boldsymbol{y}) = 0, \end{aligned} \tag{3}$$

where $\boldsymbol{y}\in C_{BS}$ and $k = 1,2$. Since the singular behavior of $\boldsymbol{\Sigma}^k(\boldsymbol{x},\boldsymbol{y};\omega)$ and $\boldsymbol{\Sigma}^k(\boldsymbol{x},\boldsymbol{y})$ is the same, the first integral over C_{BS} is regular. Granted that the displacement $\boldsymbol{u}$ satisfies the

usual assumption of Hölder continuity [2], i.e. $\boldsymbol{u} \in \mathcal{C}^{0,\alpha}$ with $0 < \alpha \leq 1$, the second integral over $C_{\varepsilon,r} + C_\varepsilon$ is weakly singular. Equation (3) is thus regularized so that it contains no worse than weakly singular integrals.

The integral equation for the crack follows immediately from an integral representation of $\boldsymbol{u}$ by applying Hooke's law and the traction-free boundary condition on the crack. The result is the integral equation:

$$\begin{aligned}\lim_{y_2 \to 0} \sigma_{i2}(y_1, y_2) = &- \int_{C_{BS}} u_j(\boldsymbol{x}) \mathcal{C}_{i2kl} \frac{\partial}{\partial y_l} \Sigma^k_{jm}(\boldsymbol{x}, y_1, 0; \omega) \mathrm{n}_m(\boldsymbol{x}) \, \mathrm{d}s_x \\ &+ \lim_{y_2 \to 0} \int_{-a}^{a} \Delta u_j(x_1) \mathcal{C}_{i2kl} \frac{\partial}{\partial y_l} \Sigma^k_{j2}(x_1, 0, y_1, y_2; \omega) \, \mathrm{d}x_1 \\ &+ \mathcal{C}_{i2kl} \frac{\partial}{\partial y_l} u^{\mathrm{in}}_k(y_1, 0) = 0,\end{aligned} \tag{4}$$

where $i = 1, 2$, $|y_1| < a$ and $\mathcal{C}_{ijkl}$ are the components of the elastic stiffness tensor $\boldsymbol{\mathcal{C}}$ in the coordinate system of the crack. It should be noted that the limit in front of the second integral cannot be moved inside the integral since the integrand is hypersingular [2, 3]. This problem is automatically resolved by the solution method, as clarified below.

PROBE MODELING

The action of the transmitting probe is modeled by prescribing the traction on the scanning surface underneath it. For the transmitting probe (t), the boundary condition on the upper surface of the component is then taken as:

$$\boldsymbol{t}^{\mathrm{b}} = \begin{cases} A_0 \mathrm{i}\mu k_p \left[\delta \sin 2\gamma \, \mathbf{e}_{x_1^{\mathrm{b}}} + \left(\frac{k_s^2}{k_p^2} - 2 \sin^2 \gamma \right) \mathbf{e}_{x_2^{\mathrm{b}}} \right] \mathrm{e}^{-\mathrm{i}k_p (x_1^{\mathrm{b}} - t_1^{\mathrm{b}}) \sin \gamma}, & \text{P probe,} \\ A_0 \mathrm{i}\mu k_s \left[-\delta \cos 2\gamma \, \mathbf{e}_{x_1^{\mathrm{b}}} + \sin 2\gamma \, \mathbf{e}_{x_2^{\mathrm{b}}} \right] \mathrm{e}^{-\mathrm{i}k_s (x_1^{\mathrm{b}} - t_1^{\mathrm{b}}) \sin \gamma}, & \text{SV probe,} \end{cases} \tag{5}$$

beneath the surface of the probe (i.e. $|x_1^{\mathrm{b}} - t_1^{\mathrm{b}}| < w_1$ and $x_2^{\mathrm{b}} = d + t_2^{\mathrm{b}}$), and $\boldsymbol{t}^{\mathrm{b}} = \mathbf{0}$ elsewhere. The two options are referred to as P probe and SV probe, respectively, since for $\delta = 1$ the traction corresponds exactly to the traction of a plane P or SV wave, respectively, restricted to the surface of the probe. The parameter δ accounts for the effect of the couplant applied between the wedge and the scanning surface: $\delta = 0$ represents fluid coupling and $\delta = 1$ a glued probe. Fluids of different viscosity can be modeled by setting an appropriate value $0 < \delta < 1$. The constant A_0 is the amplitude of the plane wave and γ is the angle of the probe, measured clockwise from the normal of the probe.

The multiple scattering between the scanning surface and the crack and back surface is neglected, so the component can be regarded as half-infinite. To determine the incoming field it can then be expanded in P and SV plane wave potentials:

$$\boldsymbol{u}^{\mathrm{in,b}}(\boldsymbol{x}^{\mathrm{b}}) = \nabla_{\mathrm{b}} \varphi(\boldsymbol{x}^{\mathrm{b}}) + \nabla_{\mathrm{b}} \times \left(\psi(\boldsymbol{x}^{\mathrm{b}}) \mathbf{e}_{x_3^{\mathrm{b}}} \right), \tag{6}$$

where ∇_{b} denotes the nabla operator in the coordinate system of the back surface and the potentials $\varphi(\boldsymbol{x}^{\mathrm{b}})$ and $\psi(\boldsymbol{x}^{\mathrm{b}})$ are given by:

$$\begin{aligned}\varphi(\boldsymbol{x}^{\mathrm{b}}) &= \frac{1}{2\pi} \int_{-\infty}^{\infty} A(q) \mathrm{e}^{\mathrm{i}(q(x_1^{\mathrm{b}} - t_1^{\mathrm{b}}) - h_p(x_2^{\mathrm{b}} - t_2^{\mathrm{b}} - d))} \, \mathrm{d}q, \\ \psi(\boldsymbol{x}^{\mathrm{b}}) &= \frac{1}{2\pi} \int_{-\infty}^{\infty} B(q) \mathrm{e}^{\mathrm{i}(q(x_1^{\mathrm{b}} - t_1^{\mathrm{b}}) - h_s(x_2^{\mathrm{b}} - t_2^{\mathrm{b}} - d))} \, \mathrm{d}q.\end{aligned} \tag{7}$$

Here $h_j = h_j(q) = \sqrt{k_j^2 - q^2}$ for $j = p, s$ and the branch of the complex square root is chosen such that $\operatorname{Im} \sqrt{z} \geq 0 \; \forall z \in \mathbb{C}$.

Identification of the Fourier transform of the traction from the incoming field given by Eq. (6) with the Fourier transform of the traction vector given by Eq. (5) yields the functions $A(q)$ and $B(q)$. This determines the incoming field from the transmitting probe.

The action of the receiving probe is modeled using the electromechanical reciprocity relation by Auld [4], which gives the change in transmission coefficient (reflection coefficient in pulse-echo testing) due to a defect. This quantity is directly proportional to the output voltage of the receiving probe. An application of the reciprocity relation to the present case gives the change in transmission coefficient due to the crack as:

$$\delta\Gamma_C = \frac{-\mathrm{i}\omega}{4P} \int_{-a}^{a} \Delta u_i(x_1) \sigma_{i2}^{\mathrm{re}}(x_1, 0) \, \mathrm{d}x_1, \tag{8}$$

and the change in transmission coefficient due to the back surface as:

$$\delta\Gamma_{BS} = \frac{\mathrm{i}\omega}{4P} \int_{C_{BS}} u_i^{\mathrm{re}}(\boldsymbol{x}) \sigma_{ij}^{\mathrm{in}}(\boldsymbol{x}) \mathrm{n}_j(\boldsymbol{x}) \, \mathrm{d}s. \tag{9}$$

In Eq. (8) and Eq. (9) the quantities u_i^{re} and $\sigma_{i2}^{\mathrm{re}}$ are the displacement and traction, respectively, in the absence of the crack but in the presence of the back surface, when the receiving probe is transmitting. The COD Δu_i is due to an incoming field from the transmitting probe, in the presence of both the crack and back surface. The stress $\sigma_{ij}^{\mathrm{in}}$ is the stress resulting from an incoming field from the transmitting probe (t), in the absence of both the crack and the back surface. It is computed by applying Hooke's law to the incoming field given by Eq. (6). The action of the receiving probe acting as a transmitter is modeled in the same way as the transmitting probe. The probes are assumed to be transmitting at the angular frequency ω, and the quantity P is essentially the power supplied to the probe in transmitting mode.

It should be noted that all the computed $\delta\Gamma$ are computed for a fixed angular frequency, i.e. $\delta\Gamma = \delta\Gamma(\omega)$. In an experimental testing situation, the quantity of interest is the signal response as measured in the time domain. To obtain the time traces, an inverse Fourier transform of $\delta\Gamma_C(\omega)$ and $\delta\Gamma_{BS}(\omega)$ is taken with the frequency spectrum:

$$\frac{4\pi}{\omega_2 - \omega_1} \sin^2\left(\pi \frac{\omega - \omega_1}{\omega_2 - \omega_1}\right) = \frac{1}{\Delta f} \cos^2\left(\pi \frac{f - f_c}{2\Delta f}\right),$$

where f_c is the center frequency and Δf the 6 dB bandwidth.

NUMERICAL SOLUTION AND EXAMPLES

To solve the coupled integral equations, three discretizations are introduced; (1): the COD Δu is expanded in a series of Chebyshev functions, (2): the back surface C_{BS} is partitioned into N_e boundary elements with N_g geometrical nodes and approximated on each element by shape functions, (3): N_i interpolation nodes on the back surface are chosen and the displacement $\Delta \boldsymbol{u}$ is approximated between the interpolation nodes on each element by interpolation functions.

Starting with the discretization of the COD $\Delta \boldsymbol{u}$, the following finite series expansion is made:

$$\Delta u_i(x_1) = \sum_{m=1}^{N} \alpha_{im} \psi_m(x_1/a), \tag{10}$$

where the truncation limit N is chosen large enough so the desired accuracy is achieved. In Eq. (10), the Chebyshev functions ψ_m are defined by:

$$\psi_m(v) = \begin{cases} \frac{1}{\pi}\cos(m \arcsin v), & m = 1, 3, \ldots, \\ \frac{\mathrm{i}}{\pi}\sin(m \arcsin v), & m = 2, 4, \ldots . \end{cases}$$

These functions form a complete orthogonal set on $[-1, 1]$ with respect to the ordinary weighted L^2-norm, with the weight function $(1 - v^2)^{-1/2}$. They also incorporate the correct square-root behavior at the crack edges and satisfy a useful integral relation.

The boundary element discretization is done in the usual way, see e.g. Bonnet [2] and Domínguez [5]. In this paper an isoparametric interpolation (i.e. the shape and interpolation functions are the same and the geometrical nodes are used also as interpolation nodes) with quadratic Lagrangian interpolation functions is used. For an isoparametric interpolation $N_i = N_g$. Letting N_{node} denote this common number, the use of quadratic interpolation functions implies that $N_{node} = 2N_e + 1$. By collocating Eq. (3) at the $2N_e + 1$ boundary node points, $2(2N_e + 1)$ linear equations are obtained. Projecting Eq. (4) on N expansion functions yields $2N$ additional linear equations. Combined, a total of $2(2N_e + 1 + N)$ equations in $2(2N_e + 1 + N)$ unknowns (the $2(2N_e + 1)$ back surface displacements and the $2N$ series expansion coefficients α_{im}) is obtained. It should be noted that the use of an isoparametrical interpolation with quadratic Lagrangian interpolation functions enforces the Hölder continuity of $\boldsymbol{u}$ which was assumed in the derivation of Eq. (3). This is essential for the effectiveness of the regularization, and leads to regular integrals which are accurately computed using ordinary Gauss-Legendre quadrature. It should also be noted that after discretizing the integral equation for the crack using the Chebyshev functions the limit in front of the hypersingular integral in Eq. (4) can be evaluated analytically, since the expansion and projection leads to convergent integrals. The resulting integrals are also straightforward to compute numerically. The regularization of the back surface integral equation and the series expansion of the COD thus results in a solution method with straightforward numerical computations and an effective treatment of the hypersingularity.

To illustrate the influence of the back surface a few numerical results are given. In the examples a pulse-echo testing situation (i.e. the same probe acting as both transmitter and receiver) is simulated and the back surface $g(x_1^{\mathrm{b}})$ is chosen as:

$$g(x_1^{\mathrm{b}}) = \begin{cases} 0, & x_1^{\mathrm{b}} < b, \\ \frac{A}{2}\left[1 + \sin\left(\frac{\pi}{c-b}\left(x_1^{\mathrm{b}} - \frac{c+b}{2}\right)\right)\right], & b \le x_1^{\mathrm{b}} \le c, \\ A, & x_1^{\mathrm{b}} > c, \end{cases}$$

where A, b, and c are defined in Fig. 1. In the numerical examples given, the parameters of the non-planar back surface are $A = 8\,\mathrm{mm}$, $b = 2\,\mathrm{mm}$ and $c = 10\,\mathrm{mm}$. The Lamé constants of the material are $\lambda = 113.2\,\mathrm{GPa}$ and $\mu = 80.9\,\mathrm{GPa}$, respectively, and the density is $\rho = 7900\,\mathrm{kg/m^3}$. A $4\,\mathrm{mm}$ wide vertical crack (i.e. $\beta = 90°$) with its center located $4\,\mathrm{mm}$ from the lower part of the back surface is considered. The probe is an $8\,\mathrm{mm}$ wide SV-probe with angle $\gamma = -45°$ and fluid coupling so that $\delta = 0$. The probe is located at a vertical distance of $15\,\mathrm{mm}$ from the center of the crack. Damping is incorporated in the model by giving the Lamé constants imaginary parts of $1\,\%$ of the real parts.

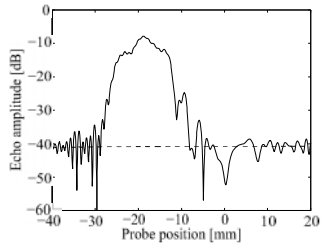

(a) Planar back surface.

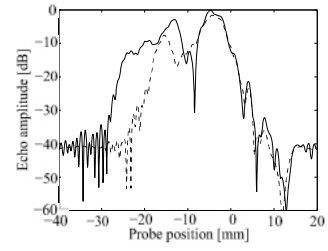

(b) Non-planar back surface.

FIGURE 2. Echo amplitudes. Solid curves (—): crack present, dashed curves (- -): crack absent.

Figure 2 shows the pulse-echo signal response as a function of probe position, computed for a single frequency of 2 MHz. The results are not calibrated, but the same normalization is used so the results can be compared. The results in Fig. 2(a) are for the planar back surface, those in Fig. 2(b) for the non-planar back surface. In both figures the dashed curve shows the signal response from the back surface in the absence of the crack, and the full-drawn curve shows the total signal response with the crack present. As seen in Fig. 2(a), the planar back surface gives only a very weak signal response which is also independent of probe position, as expected. Figure 2 also shows strong corner echoes from the crack, as expected.

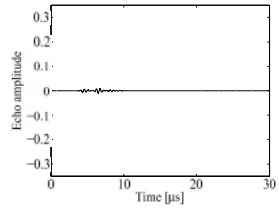

(a) Planar back surface, crack absent.

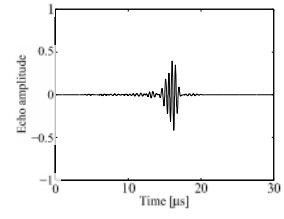

(b) Planar back surface, crack present.

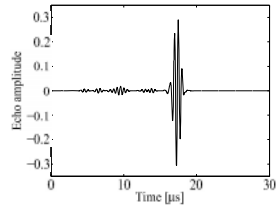

(c) Non-planar back surface, crack absent.

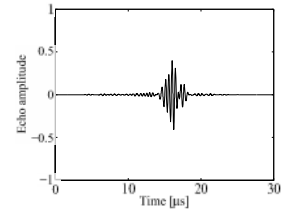

(d) Non-planar back surface, crack present.

FIGURE 3. Time traces for a probe located 17.4 mm to the left of the crack.

Figure 3 shows the time traces for a probe positioned 17.4 mm to the left of the crack center, computed for a center frequency $f_c = 2$ MHz and 6 dB bandwidth $\Delta f = 1$ MHz. The normalization is the same in all time traces, but it should be noted that the scale is different in the time traces without and with the crack present.

As can be seen both in Fig. 2(b) and by comparing Fig. 3(c) and 3(d), for a probe positioned around 17 mm to the left of the crack center the signal amplitude is approximately equal with and without the crack. In addition, the strong pure SV-wave pulse from the crack arriving at $t \approx 16.1$ μs in the time traces in Fig. 3(d) is only just distinguishable from the strong pure SV-wave pulse from the back surface arriving at $t \approx 17.4$ μs. Even for this very simple geometry and favorable testing situation there are thus probe positions for which a crack may be quite difficult to detect, when the back surface is non-planar.

CONCLUSIONS

In this paper a 2D model of ultrasonic testing for interior strip-like cracks near a non-planar back surface is developed. The incident field emitted from an ultrasonic contact probe is modeled by prescribing the traction on the component beneath the probe. This enables the derivation of an explicit expression for the incident field in terms of an inverse Fourier transform. The wave scattering problem is solved by reformulating it as two coupled boundary integral equations for the unknown crack opening and back surface displacements. By using a combination of a series expansion of the COD and a boundary element discretization of the back surface to solve the coupled integral equations, the hypersingularity in the BIE for the crack can be treated analytically while the geometry of the back surface is allowed to be quite general. The model is completed by employing an electromechanical reciprocity relation to model the action of the receiving probe and applying an inverse temporal Fourier transform to obtain the time traces.

Work on an extension of the present model to the 3D case with a rectangular crack is in progress, and future work will treat also other defects.

ACKNOWLEDGMENT

The present work is sponsored by the Swedish Radiation Safety Authority (SSM) and this is gratefully acknowledged.

REFERENCES

1. J. Westlund, *Review of Progress in Quantitative Nondestructive Evaluation* **28A**, 81-88 (2009).
2. M. Bonnet, *Boundary Integral Equation Methods for Solids and Fluids*, John Wiley & Sons Ltd, Chichester, 1995.
3. P.A. Martin and F.J. Rizzo, *Int. J. Numer. Methods Eng.* **39**, 687-704 (1996).
4. B.A. Auld, *Wave Motion* **1**, 3-10 (1979).
5. J. Domínguez, *Boundary Elements in Dynamics*, Computational Mechanics Publications, Southampton, 1993.